first break volume 29, July 2011

Analysis of vibrator performance at low frequencies

Zhouhong Wei[1*] and Thomas F. Phillips[1]

Abstract

It has been recognized that extending the bandwidth of seismic measurements below 10 Hz can bring many benefits for geophysical exploration. Due to physical limitations in vibrator mechanical and hydraulic systems, the ability of seismic vibrators to produce significant output power at low frequencies is limited. This paper focuses on the key factors that limit vibrator performance at low frequencies and demonstrates them empirically. Our main purpose is to help geophysicists understand seismic vibrator performance at low frequencies so that they can design an optimal low frequency sweep.

Introduction

Increasing the low-frequency content in the seismic spectrum has gained much attention in recent years (Mougenot, 2006; Bagaini, 2006, 2008; Baeten et al., 2010). There are several reasons for this: to image deep targets, to improve accuracy in the inversion of seismic data to acoustic impedance, and to enable waveform inversion for the determination or refinement of a velocity model. Due to mechanical and hydraulic constraints, it is difficult for seismic vibrators to produce sufficient force for transmission of seismic energy into the ground below about 10 Hz. Furthermore, due to non-linear effects in the vibrator hydraulics and the low rigidity of the baseplate, the low-frequency ground force contains substantial harmonic components.

Bagaini (2006) designed a maximum-displacement sweep to generate the maximum possible ground force from a seismic vibrator. He considered that at low frequencies, from 5 Hz to 8 Hz in modern seismic vibrators, the maximum travel distance, or stroke, of the reaction mass limits the energy that can be transmitted to the ground. The maximum-displacement sweeps are designed using the value of the displacement limit frequency at which the maximum driving force can be used without exceeding the maximal displacement of the reaction mass. A maximum-displacement sweep has a variable sweep rate and an optimally designed driving force envelope that permit the transmission to the ground of the maximum energy, given the vibrator's mechanical and hydraulic constraints. In a later article, Bagaini (2008) stated that the vibrator ground force output is limited by the maximum displacement of the reaction mass at the low frequencies, from 3 Hz to 8 Hz. Meanwhile, he demonstrated that the harmonic distortion at low frequencies is also a factor that limits the energy radiated into ground at the fundamental frequency. Therefore, the effect of harmonic distortion is also incorporated into the maximum-displacement sweep design.

Sallas (2010) reviewed almost all the hydraulic and mechanical constraints in a modern seismic vibrator that physically limit the maximum ground force produced by the vibrator. He demonstrated that the ground force at low frequencies, below 10 Hz, is actually limited by a combination of the reaction-mass maximum displacement and the maximum pump flow rate. Considering these limits, he gave a sweep-rate formula to show how a low-frequency sweep can be designed.

Wei et al. (2007) studied theoretically vibrator performance at frequencies below 20 Hz. It was found using simulation model data that the ground force produced from a seismic vibrator is constrained by several mechanical and hydraulic limitations: the reaction-mass stroke, the hydraulic pump flow rate, the pump response time, the servo-valve stroke, the accumulator size, the engine horsepower, the peak-decoupling force, the harmonic distortion, and the vehicle chassis isolation.

The peak-decoupling force is the smaller of the theoretical hydraulic force and the hold-down weight. The theoretical hydraulic force is equal to the hydraulic supply pressure multiplied by the piston area in the reaction mass chamber. The vibrator hold-down weight is the weight of the vibrator vehicle upon which the actuator is installed. For a modern seismic vibrator, the hydraulic supply pressure is normally set as 3000 psi (207 bar) while the piston area varies and depends on the model of the vibrator and the vibrator manufacturers. For an AHV-IV model 362 vibrator, the piston area is 20.6 in^2 (132.9 cm^2). Thus, the theoretical hydraulic force is calculated to be 61,800

---

[1] *INOVA Geophysical Equipment, 12200 Parc Crest Drive, Stafford, TX77477, USA.*

[*] *Corresponding author, E-mail: john.wei@inovageo.com*

lbf (274,886.4 N). For this type of vibrator model, the hold-down weight is 64,000 lbf (284,672 N). Therefore, the peak-decoupling force equals the theoretical hydraulic force.

Among the mechanical and hydraulic limiting factors, the reaction-mass stroke and the peak-decoupling force are two key parameters for limiting the vibrator ground force at the fundamental frequency that can be achieved at low frequencies. It was also discovered that there is a bounding frequency dependent on the reaction mass in the vibrator system. For example, for the AHV-IV model 362 vibrator (standard vibrator), this bounding frequency is ~5 Hz, while for the AHV-IV model 364 vibrator (modified vibrator) this frequency is ~4 Hz. Below this bounding frequency the vibrator output is limited by the reaction-mass stroke, while above the boundary frequency the vibrator force output is limited by the peak-decoupling force.

Wei (2008a) presented empirical results of vibrator performance at low frequencies using monochromatic frequency sweeps. The results supported the previous theoretical work on low-frequency performance. Wei (2009) made a study of vibrator performance at low frequencies based on an enhanced standard vibrator, carrying a heavier mass of 5003 kg. He also provided some basic equations for calculating the ground force output from a vibrator at the fundamental frequency in the frequency range 2–8 Hz.

In order to evaluate vibrator performance at low frequencies, a field test was carried out using a modified vibrator to shake with monochromatic frequency sweeps. The monochromatic frequency sweep was chosen to enable an accurate evaluation on the ground force that can be maximally output from a vibrator. The sweep length of each monochromatic frequency sweep was 5 s to ensure that steady-state performance of the vibrator was achieved. In this test, the vibrator was placed on load cells and performed at frequencies of 1.5 Hz, 2 Hz, 2.5 Hz, 3 Hz, 4 Hz, 5 Hz, 6 Hz, 7 Hz, and 8 Hz at theoretically calculated force levels.

Using load cells, the vibrator true ground force can be measured. In total, there are eight load cells evenly distributed beneath the baseplate, and these load cells are firmly mounted on a concrete pad. The baseplate is coupled with the concrete only through these load cells. Since the area of each load cell is very small, the coupling between the baseplate and the concrete becomes a point-loading condition at each load cell. Therefore, the coupling between the baseplate and the concrete is very poor. With such poor loading conditions, the effect on the vibrator ground force output due to baseplate bending can be evaluated. The baseplate bending could be the reason why such a strong second harmonic is produced at low frequencies.

Data acquisition for the vibrator in the test was handled with a National Instruments 32-channel system utilizing Lab View software. During vibrator testing, four control limits, the servo-valve displacement limit, the reaction-mass displacement limit, the reaction-mass force limit, and the peak force limit were all set to 100% in the control electronics. For example, both the reaction-mass force limit and the peak force limit were set to be 61,800 lbf (274 kN).

Theory

At low frequencies below the resonance of the baseplate and ground, the ground force output from a vibrator is dominated by the reaction-mass force (the hydraulic force) and can be expressed as (Wei et al., 2010)

$$F = MA\,, \tag{1}$$

where F is the ground force, M is the mass of the reaction mass, and A is the acceleration of the reaction mass. The resonance of the baseplate and ground normally lies within the frequency range 15–35 Hz, and depends on the ground stiffness, the mass of the baseplate, and the mass of the captured ground (Wei, 2008b). The captured ground mass is the ground mass that is seen by the vibrator baseplate. If good coupling is achieved between the baseplate and the ground, the captured ground mass participates with the same motion as the baseplate and becomes a part of source. In general, Equation (1) is an accurate representation of the vibrator ground force at frequencies below 10 Hz. Because sinusoidal sweeps are used to operate the vibrator, the reaction mass acceleration at a single frequency, f, can be expressed as

$$A = -4\pi^2 Xf^2 \sin 2\pi ft\,, \tag{2}$$

where X is the amplitude of the reaction-mass displacement and t is time. Therefore, the maximum acceleration of the reaction mass is

$$A_{\max} = -4\pi^2 Xf^2\,. \tag{3}$$

Combining Equations (1) and (3), the peak vibrator ground force is theoretically

$$F = 4\pi^2 MXf^2\,. \tag{4}$$

This peak ground force can be produced if the vibrator is a perfect machine. At low frequencies, where X is constant because it is the maximum displacement of the reaction mass, the theoretical peak ground force is proportional to the square of the frequency. The constant of proportionality is determined by the magnitude of the reaction mass and its maximum displacement. For example, in the modified vibrator M is 11,020 lb (4959 kg) and X is 1.95 in (4.95 cm). Equation (4) further shows that increasing the reaction mass and the stroke are the only ways to increase the ground force at low frequencies. However, these changes would require the vibrator hydraulic components, for example, the engine, the hydraulic pump, the servo-valves, accumulators, and hoses to be significantly enlarged such that it becomes difficult and costly to build the vibrator (Gibson et al., 2010).

Figure 1 shows the vibrator ground force profiles from 1.5 Hz to 8 Hz produced by the modified vibrator. The green curve depicts the envelope of the theoretical ground force, based on Equation (4), that the modified vibrator can produce. This theoretical force is a pure fundamental frequency component. The blue curve is the force measured by load cells after filtering out the harmonic distortion, so it is the amplitude of the fundamental frequency component actually output from the modified vibrator. The theoretical ground force increases as the frequency increases. Theoretically, the vibrator can produce a ground force of 42,000 lbf (186 kN) at 4 Hz, over 70% of the hydraulic force, and 61,800 lbf (274 kN) at 5 Hz, 100% of hydraulic force. However, in practice, the ground force output from the vibrator is significantly less than the theoretically predicted ground force, and the vibrator can never achieve 100% of the hydraulic force. At approximately 7 Hz, the vibrator ground force reaches 70% of the hydraulic force. The obvious question is: what offsets the rest of the hydraulic force?

In order to address this question, vibrator measurements such as the peak force, the ground force at the fundamental frequency, and the reaction mass displacement are presented below for comparison. The peak force is the maximum ground force that is actually output from the vibrator. This force is a function of time and contains severe harmonic distortion. The ground force at the fundamental frequency, often referred to as the fundamental force, was obtained for each monochromatic frequency sweep by removing most of the harmonic content from the peak force using a time-variant filter. All of the displays are shown in the time domain as wiggle traces.

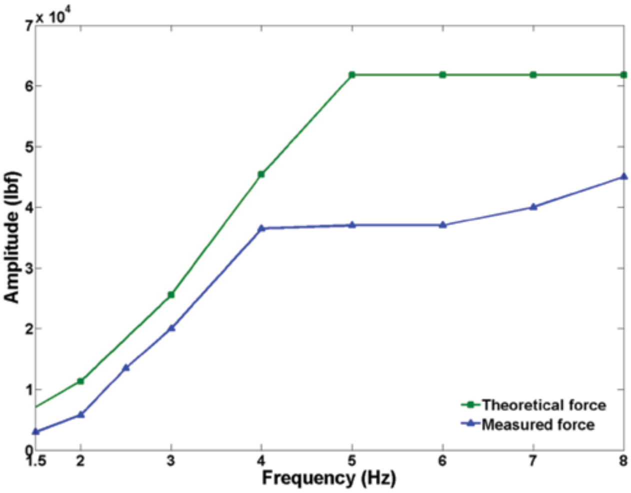

Figure 1 *The vibrator ground force envelope at low frequencies.*

Data and analysis from 1.5 Hz to 3 Hz

Figure 2 shows comparisons of fundamental force and peak force at 1.5 Hz and 2 Hz produced by the modified vibrator on load cells. It can be seen (Figure 2a) that the vibrator only outputs a fundamental force of 3300 lbf at 1.5 Hz, although theoretically (Figure 1) the vibrator is supposed to produce a fundamental force of 7100 lbf. Figure 2b shows that at 2 Hz the vibrator actually produces a fundamental force of about 5800 lbf, whereas the theory predicts that the vibrator should produce a fundamental force of 11,000 lbf.

There is a trough at each half cycle in the peak force (Figure 2a). These troughs indicate that the peak force contains significant odd harmonics dominated by the third harmonic. The trough shape in the lower half-cycle is not as symmetrical as the trough shape in the upper half-cycle. This difference in shape implies that the peak force also contains a certain amount of even harmonics, dominated by the second harmonic. The amplitude of each trough in a half-cycle is estimated as approximately 3500 lbf. Summing with the fundamental force amplitude of 3300 lbf gives 6800 lbf. This summed force amplitude is very close to the theoretical force (7100 lbf) shown in Figure 1.

The peak force in Figure 2b looks very similar to that in Figure 2a. The average amplitude of the trough in each cycle is approximately 5000 lbf. With the fundamental force amplitude of 5800 lbf, the summed amplitude is

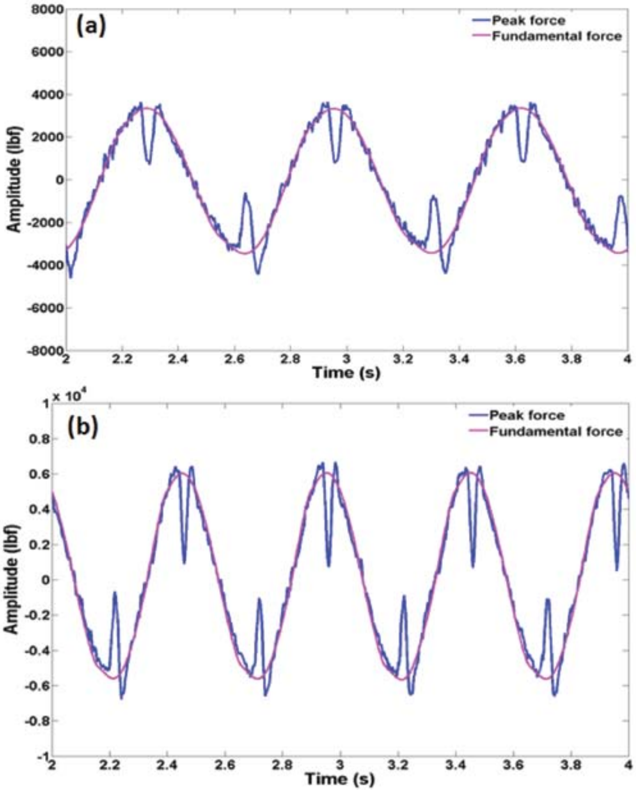

Figure 2 *The peak force and fundamental force output from a vibrator at (a) 1.5 Hz; (b) 2 Hz.*

10,800 lbf, closely matching the theoretical force of 11,000 lbf calculated at 2 Hz. Based on Figure 2, it can be concluded that there are non-linearities in the vibrator system that cause approximately 50% of the theoretical force to produce harmonic troughs instead of force at the fundamental frequency.

Figure 3 shows the reaction mass displacements when the vibrator vibrates at 1.5 Hz and 2 Hz. Both reaction mass displacements are very close to the maximal travel limit of 1.96 in (4.98 cm). This means that the vibrator follows the commands given by the control electronics very well. Unfortunately, the reaction-mass movements are constrained by the maximally available travel distance. Therefore, the ground force as given by Equation (4) is limited.

Figure 4 shows comparisons of fundamental force and peak force at 2.5 Hz and 3 Hz produced by the modified vibrator on load cells. The vibrator actually produces fundamental forces of about 13,500 lbf and 22,000 lbf at 2.5 Hz and 3 Hz, respectively, while theoretically it should generate about 18,450 lbf and 25,556 lbf of fundamental force at these frequencies. The reaction-mass displacements almost reach the maximal travel limit (Figure 5), as at 1.5 Hz and 2 Hz (Figure 3).

In Figure 4a, there are both a peak and a trough in the upper half-cycle of the peak force, whereas there is only a trough in the lower half-cycle. The amplitude of this peak-and-trough contribution to the peak force is approximately 4500 lbf. Again, adding this amplitude to the fundamental force amplitude of 13,500 lbf gives a sum close to the theoretically predicted force (18,450 lbf). In contrast to the behaviour at 2.5 Hz (Figure 4a), at 3 Hz peaks instead of troughs appear in both the upper and lower half-cycles of the peak-force (Figure 4b). Evidently, the peaks in the upper and lower half-cycles are not symmetrical. The amplitude at the fundamental frequency is about 22,000 lbf, which is 14% less than the theoretical force of 25,556 lbf. However, the summed amplitudes of the peak force at the fundamental frequency and harmonics produced by the vibrator is approximately equivalent to the theoretical force. Again, it can be concluded from Figure 4 that harmonic distortion takes away a significant amount of force which theoretically belongs to the fundamental force.

Wei and Phillips (2010) discussed four non-linearities in the vibrator system. Among these non-linearities, the servo-valve characteristics near null, frequently referred to as the dead band or overlap of the main-stage servo-valve, are the main source of the troughs that appear in the peak force (Figures 2 and 4). This type of non-linearity dominates

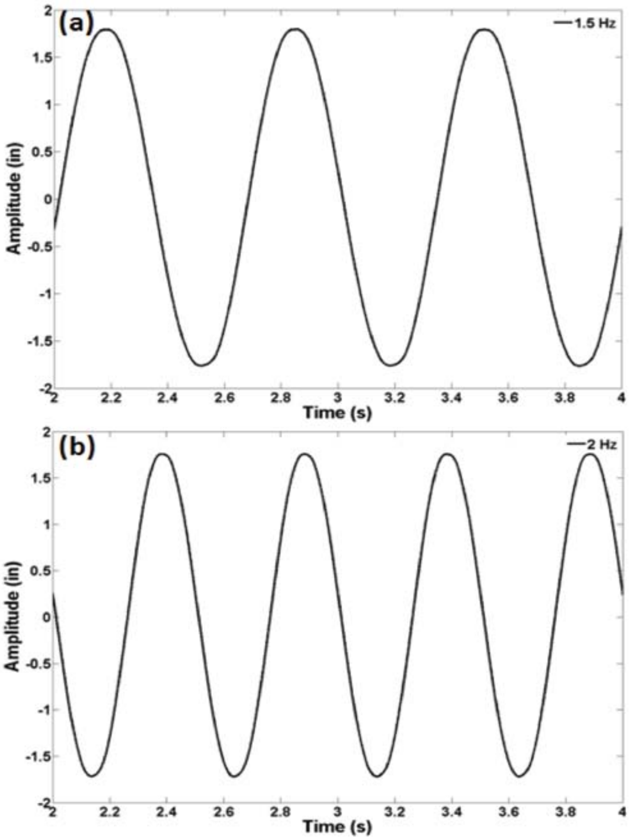

Figure 3 *The vibrator reaction-mass displacement at (a) 1.5 Hz; (b) 2 Hz.*

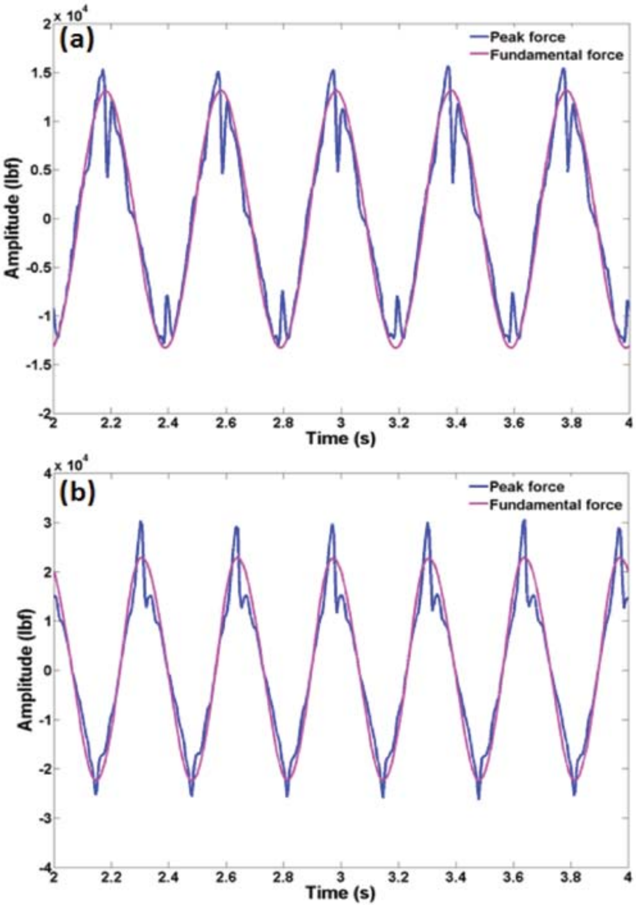

Figure 4 *The peak force and fundamental force output from a vibrator at (a) 2.5 Hz; (b) 3 Hz.*

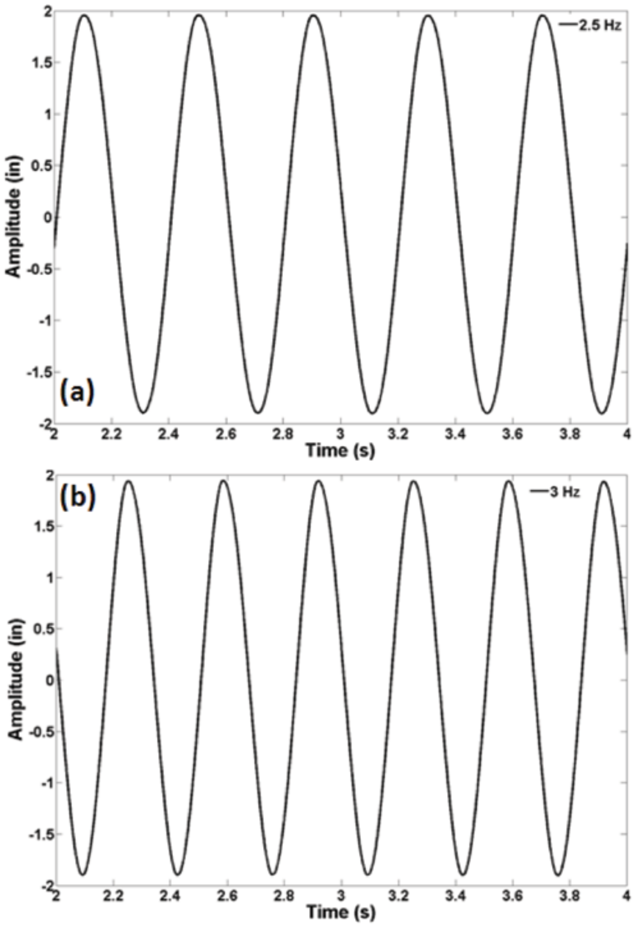

Figure 5 The vibrator reaction-mass displacement at (a) 2.5 Hz; (b) 3 Hz.

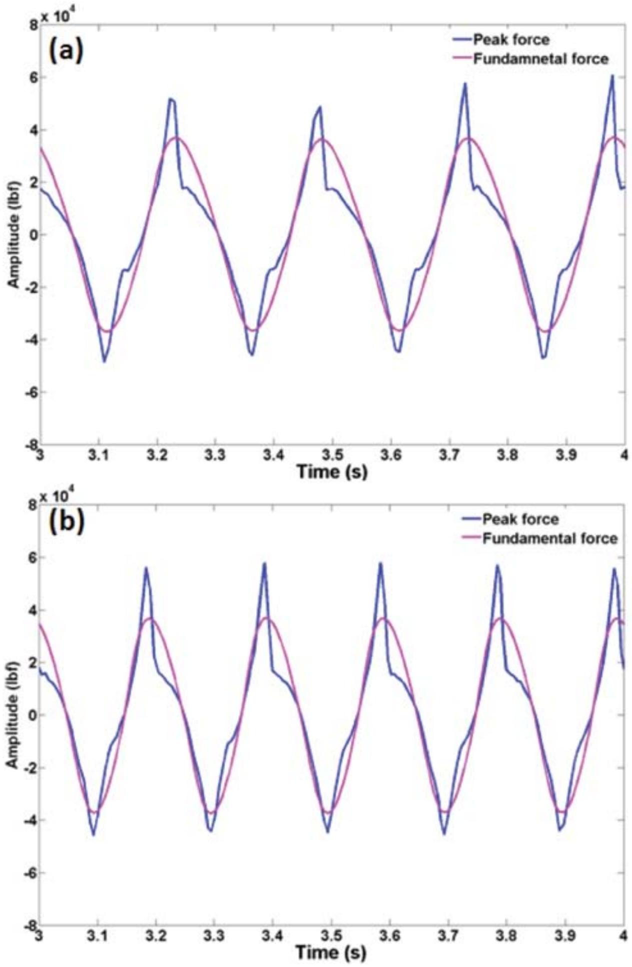

Figure 6 The peak force and fundamental force output from a vibrator at (a) 4 Hz; (b) 5 Hz.

when the vibrator vibrates at very low frequencies as well as at low force outputs. Under this non-linearity, significant odd harmonics dominated by the third harmonic are produced (Garagić and Srinivasan, 2004). Additionally, this non-linearity will cause the waveform to notch at its peak. Meanwhile, due to low rigidity of the vibrator baseplate, the non-linear contact-stiffness between the vibrator baseplate and the ground creates even harmonics dominated by the second harmonic (Wei, 2010). Wei et al. (2010) demonstrated that at low frequencies the non-linear contact-stiffness between the baseplate and the ground could cause asymmetrical flows and volumes in the reaction-mass chamber. These asymmetries of flows and volumes in the reaction-mass chamber will result in even harmonics, dominated by the second harmonic.

Apart from non-linearity of the servo-valve dead band, there is another non-linearity, referred to as servo-valve non-linear flow-pressure characteristics, in the vibrator servo-valve system (Merritt, 1967; Wei and Phillips, 2010). This non-linearity becomes dominant when the vibrator shakes at frequencies above 3 Hz with high force outputs. The more force the vibrator outputs, the more the flow-pressure non-linearity is yielded. In general, this non-linearity will create significant odd harmonics dominated by the third and fifth harmonics (Wei and Phillips, 2010). Moreover, this non-linearity intends to peak the waveform of the ground force to give it a triangular shape. Additionally, as explained earlier, the vibrator ground force still suffers even harmonics due to low rigidity of the vibrator baseplate. From 2.5 Hz to 3 Hz, the dominant non-linearity is transferred from the servo-valve dead band to the non-linear flow-pressure relationship.

Data and analysis from 4 Hz to 8 Hz

Figure 6 shows comparisons of fundamental force and peak force at 4 Hz and 5 Hz produced by the modified vibrator on load cells. It can be seen that the peak force waveforms produced by the vibrator are close to triangular, with the upper half-cycles being more sharply peaked than the lower half-cycles. Also, it can be observed that the maximum peak value in each upper half-cycle almost reaches the peak force limit setting (61,800 lbf). However, the vibrator actually produces a fundamental force of 37,000 lbf at 4 and 5 Hz, although the theoretical fundamental forces are 45,333 lbf and 61,800 lbf at the respective frequencies. Obviously, there are big discrepancies between the measured forces and the theoretically predicted forces.

Figure 7 shows the reaction-mass displacements at 4 Hz and 5 Hz. At 4 Hz, the reaction-mass displacement is again close to the maximal travel limit, just as it is at frequencies below 3 Hz. However, the reaction-mass displacement at 5 Hz decreases dramatically. This means that at frequencies above 4 Hz the reaction-mass maximum travel distance no longer restrains the vibrator force output.

Figure 8 shows comparisons of fundamental force and peak force at 6 Hz and 8 Hz. Similar to Figure 6, the waveforms of the peak forces are approximately triangular. The upper half-cycle is sharper than the lower half cycle. Peak amplitudes in upper half-cycles at both frequencies reach the peak force limit setting (61,800 lbf). A large discrepancy between the fundamental force and the theoretically predicted force is also observed. Compared with the reaction-mass displacement at 5 Hz (Figure 7b), the reaction-mass displacements measured at 6 Hz and 8 Hz (Figure 9) are far below the maximal reaction-mass travel limit.

Comparing Figures 6 and 8, the peak force output from the vibrator can be seen to be triangular at 4 Hz, unlike the peak forces with troughs shown in Figure 2. Furthermore, the peak force limit is reached at frequencies above 4 Hz, meaning that the vibrator output is restricted by the peak-decoupling force to avoid complete decoupling. These observations indicate that there is a boundary of frequency at 4 Hz in the vibrator system. Below this boundary frequency, the vibrator force output is constrained by the reaction-mass maximum travel distance, while above this frequency the reaction-mass maximum travel displacement is not a limiting factor on the vibrator force output. Instead, the peak-decoupling force restricts the vibrator force output and becomes the limiting factor.

As mentioned earlier, the non-linearity of servo-valve flow-pressure characteristics becomes dominant when the vibrator shakes at high frequencies as well as at high force outputs. This non-linearity becomes much stronger when the vibrator increases its output forces. It is this non-linearity in the servo-valve that causes severe odd harmonics to peak the vibrator output force, and eventually to reach the peak force limit. Therefore, at 4 Hz and above the vibrator cannot generate enough required fundamental force, and force is wasted in producing harmonic distortion.

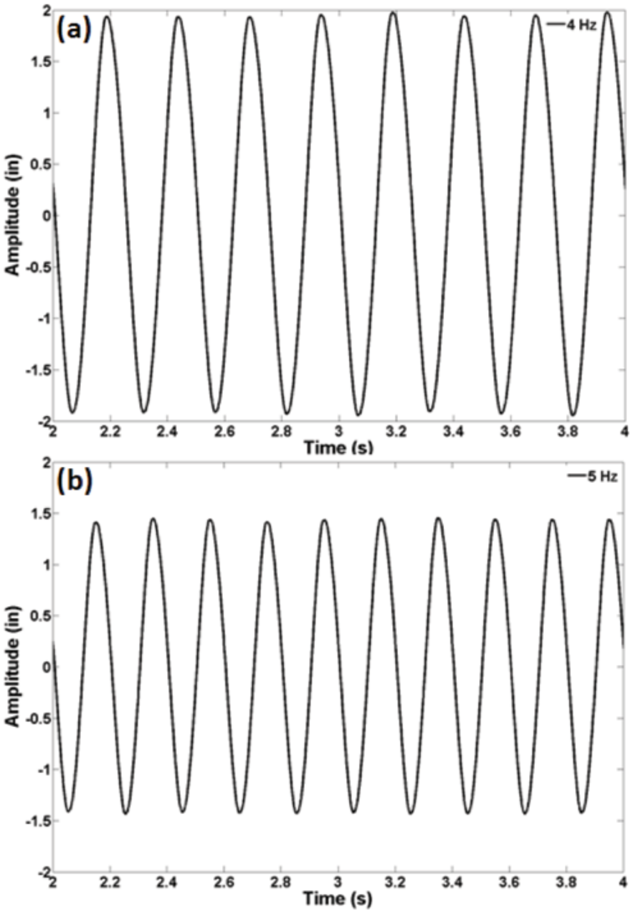

Figure 7 The vibrator reaction-mass displacement at (a) 4 Hz; (b) 5 Hz.

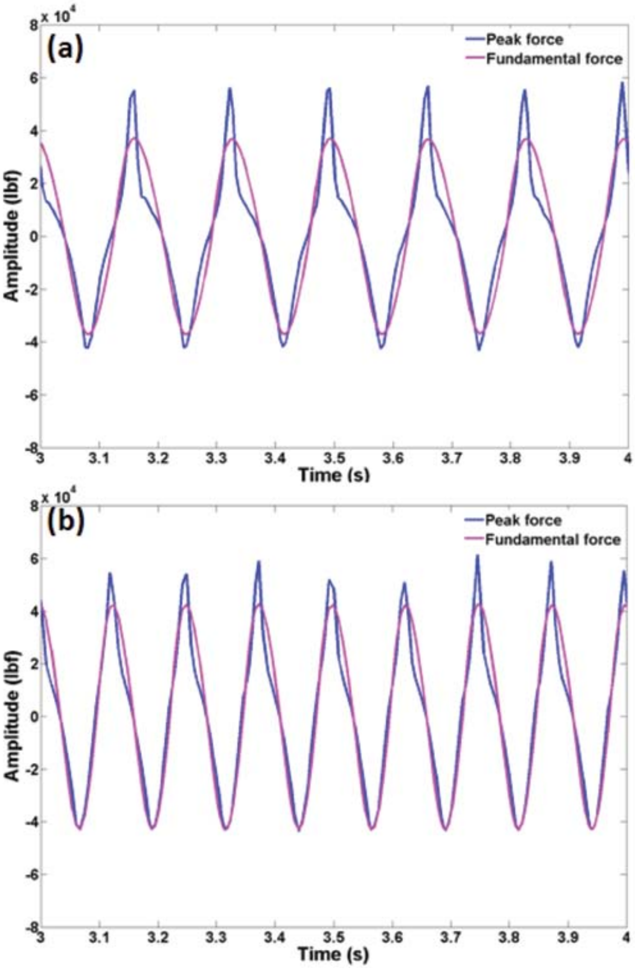

Figure 8 The peak force and fundamental force output from a vibrator at (a) 6 Hz; (b) 8 Hz.

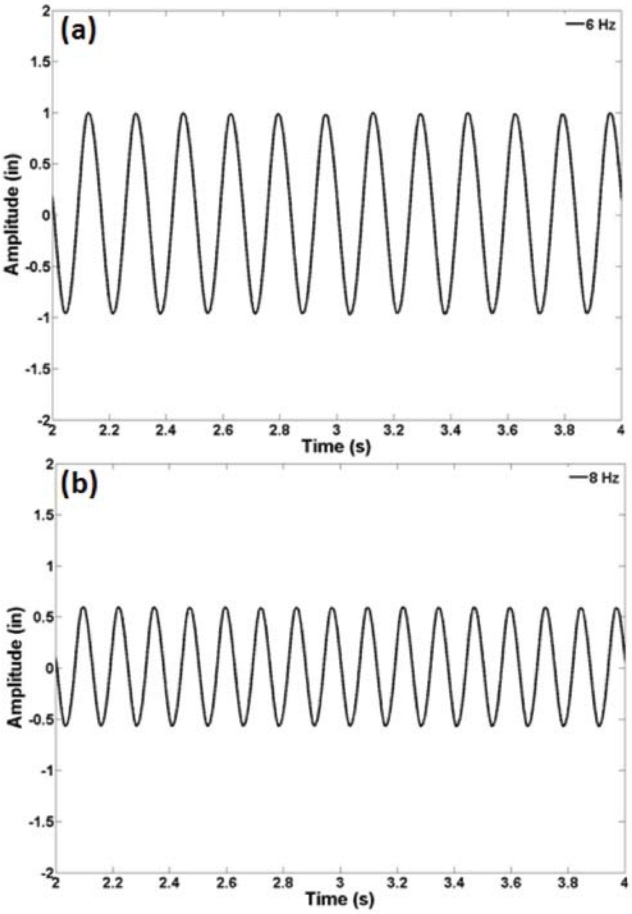

***Figure 9** The vibrator reaction-mass displacement at (a) 6 Hz; (b) 8 Hz.*

Conclusions

In general, the vibrator ground force output at frequencies below 10 Hz is restricted by two limiting factors. There is a boundary of frequency at 4 Hz in the vibrator system. Below this boundary, the vibrator force output is limited by the reaction-mass maximum travel distance. Above this boundary, the peak force limit constrains the vibrator force output. The harmonic distortion can be treated as an additional limit that results in less fundamental force being produced by the vibrator. There are two different non-linear mechanisms that are extremely effective at low frequencies. Below 3 Hz the non-linearity of servo-valve dead band controls and causes harmonic troughs in the vibrator output force, while above 4 Hz the non-linearity of servo-valve flow-pressure characteristics is so dominant that the vibrator output force becomes triangular. From 3 Hz to 4 Hz the vibrator output force is affected by both non-linearities.

References

Baeten, G., Egreteau, A., Gibson, J., Lin, F., Maxwell, P. and Sallas, J. [2010] Low-frequency generation using seismic vibrators. *72nd EAGE Conference & Exhibition*, Extended Abstracts, B015.

Bagaini, C. [2006] Enhancing the low-frequency content of Vibroseis data. *76th SEG Annual Meeting*, Expanded Abstracts, **25**, 75–79.

Bagaini, C. [2008] Low-frequency Vibroseis data with maximum displacement sweeps. *The Leading Edge*, **27**, 582–591.

Garagić, D. and Srinivasan, K. [2004] Application of nonlinear adaptive control techniques to an electrohydraulic velocity servomechanism. *IEEE Transactions on Control System Technology*, **12**, 303–314.

Gibson, J., Sallas, J.J. and Baeten, G. [2010] Pushing Vibroseis to lower frequency. *SEG/EAGE Summer Research Workshop*, Snowbird, Utah.

Merritt, H.E. [1967] *Hydraulic Control Systems*. Wiley, New York.

Mougenot, D. [2006] Toward the low frequencies: land and marine equipment. *First Break*, **24**(7), 37–41.

Sallas, J.J. [2010] How do hydraulic vibrators work? A look inside the black box. *Geophysical Prospecting*, **58**, 3–17.

Wei, Z. [2008a] Pushing the vibrator envelope: extending low and high frequency limits. *First Break*, **26**(3), 37–43.

Wei, Z. [2008b] Design of a P-wave seismic vibrator with advanced performance. *GeoArabia*, **13**, 123–136.

Wei, Z. [2009] Pushing the vibrator ground-force envelope towards low frequencies. *Geophysical Prospecting*, **57**, 151–161.

Wei, Z. [2010] Modeling and modal analysis of seismic vibrator baseplate. *Geophysical Prospecting*, **58**, 19–32.

Wei, Z. and Phillips, T.F. [2010] Harmonic distortion reduction on seismic vibrators. *The Leading Edge*, **29**, 256–261.

Wei, Z., Phillips, T.F. and Hall, M.A. [2010] Fundamental discussions on seismic vibrators. *Geophysics*, **75**, W13–W25.

Wei, Z., Sallas, J. and Tite, G. [2007] Pushing the vibrator envelope – how low can we go? *69th EAGE Conference & Exhibition*, Extended Abstracts, P183.

Received 11 February 2011; accepted 1 May 2011.
doi: 10.3997/1365-2397.2011020


EAGE
EUROPEAN ASSOCIATION OF GEOSCIENTISTS & ENGINEERS
Near Surface 2011
Register Now!
www.eage.org
12-14 September 2011, Leicester, UK